DOI 10.1002/pmic.200700026 *Proteomics* 2007, *7*, 2522–2529

RESEARCH ARTICLE

A combination of neutral loss and targeted product ion scanning with two enzymatic digestions facilitates the comprehensive mapping of phosphorylation sites

Juan Casado-Vela[1], Edgar J. Ruiz[2], Angel R. Nebreda[2] and J. Ignacio Casal[1]

[1] Protein Technology Unit, Biotechnology Programme, Spanish National Cancer Centre, CNIO, Madrid, Spain
[2] Signalling and Cell Cycle Group, Molecular Oncology Programme, Spanish National Cancer Centre, CNIO, Madrid, Spain

Received: January 10, 2007
Revised: May 4, 2007
Accepted: May 9, 2007

We propose here a new strategy for the exhaustive mapping of phosphorylation sites in the *Xenopus laevis* Cdc25 phosphatase, which regulates cell cycle progression in eukaryotic cells. Two different MS analyses in a linear IT were used to identify the phosphorylated residues. First, a data-dependent neutral loss (DDNL) analysis triggered the fragmentation of peptides that show enhanced neutral loss of phosphoric acid. Second, a targeted product ion scanning (TPIS) mass analysis was carried out in which MS^2 events are triggered for specific m/z values. Full coverage of the protein sequence was obtained by combining the two analyses with two enzymatic digestions, trypsin and chymotrypsin, yielding a comprehensive map of the phosphorylation sites. Previous reports have shown Cdc25C to be phosphorylated by Cdc2–cyclin B at four residues (Thr^{48}, Thr^{67}, Thr^{138} and Ser^{205}). By using this combination of scan modes, we have identified four additional phosphorylation sites (Thr^{86}, Ser^{99}, Thr^{112} and Ser^{163}) in a recombinant Cdc25C protein containing 198 residues of the NH_2-terminal noncatalytic domain. The sensitivity of this combined approach makes it extremely useful for the comprehensive characterization of phosphorylation sites, virtually permitting complete coverage of the protein sequence with peptides within the mass detection range of the linear IT.

Keywords:
Cdc25 / Linear ion trap / Neutral loss / Phosphorylation analysis / TPIS

1 Introduction

Phosphorylation is one of the most important and most common ways of regulating biological processes, such as the cell cycle [1, 2]. An analysis of phosphorylation can be carried out by cleaving proteins into their constituent peptides through endopeptidase digestion, generally using trypsin, and by separating and analysing the resulting peptides by HPLC-MS/MS [3]. The high sensitivity and the ability to isolate and fragment peptides in MS^n ion trapping events serve as a quick and reliable method to detect phosphorylation as well as other PTMs [4–6]. Therefore, the use of nano-HPLC (n-HPLC) coupled to a linear IT with high ion capacity and scan rates [7] enhances the detection of phosphorylated peptides and enables the phosphorylation of specific residues to be determined [8, 9]. However, the m/z detection limit range currently used for peptide fragmentation in linear ITs is normally between 400 and 2000. This limitation represents a problem when using a single enzyme like trypsin for the digestion, which may leave relatively large peptides. We

Correspondence: Dr. J. Ignacio Casal, Protein Technology Unit, Biotechnology Programme, Spanish National Cancer Centre, CNIO, Madrid, Spain
E-mail: icasal@cnio.es; http://www.cnio.es
Fax: +34-912246972

Abbreviations: DDNL, data-dependent neutral loss; **MPF,** M-phase promoting factor; **n-HPLC,** nano-HPLC; **TPIS,** targeted product ion scanning

anticipate that the controlled use of a more promiscuous enzyme like chymotrypsin would facilitate the recovery of peptides within a more appropriate m/z range and would increase the sequence coverage of the analysed protein.

In order to detect phosphorylation sites on protein digests, data-dependent mass analyses are frequently used to trigger MS^3 scans when specific neutral losses (98.0, 49.0 and 32.7 Da) are observed [10]. This analysis is known as data-dependent neutral loss (DDNL). Nevertheless, MS analysis of phosphorylated peptides must overcome several problems: (i) phosphopeptides are present at low stoichiometry in the peptide mixture; (ii) there is an increased risk of losing phosphopeptides in the RP column; (iii) a selective ionization suppression of the phosphopeptides might occur [11]. For these reasons, the development of more sensitive approaches to selectively identify and characterize phosphopeptides from the digestion mixtures is highly desirable. In this sense, targeted product ion scanning (TPIS) analysis [12] permits the selective fragmentation of certain preselected ions with the expected mass increase (+80 Da), and it favours the identification and characterization of phosphopeptides [6].

As a biological model to test the combination of these different approaches, we have studied the *in vitro* phosphorylation of *Xenopus* Cdc25C by Cdc2–cyclin B. The Cdc25 protein family includes three members, Cdc25A, Cdc25B and Cdc25C [13, 14], which dephosphorylate specific Tyr and Thr residues on cyclin-dependent kinases (CDKs). The activity of Cdc25 phosphatases is modulated by the phosphorylation of multiple sites that is in turn catalysed by several protein kinases [15, 16]. Cdc25C promotes the G_2/M transition through the activation of the M-phase promoting factor (MPF)[14], a main component of which is the Cdc2–cyclin B complex. The activation of Cdc25C during *Xenopus* oocyte maturation correlates with its phosphorylation at multiple sites located in the amino-terminal noncatalytic domain [17]. The ability of active Cdc2–cyclin B to phosphorylate Cdc25C, which can then dephosphorylate and activate more Cdc2–cyclin B complexes, forms an autocatalytic feedback loop that may ensure sufficient MPF activity required to drive *Xenopus* oocytes through M-phase [17, 18]. In order to characterise these cell cycle regulatory mechanisms, it is important to elucidate the exact location of the residues phosphorylated in Cdc25C. Previous site directed mutagenesis analysis have shown that Thr^{48}, Thr^{67}, Thr^{138} and Ser^{205} contribute to the overall phosphorylation of *Xenopus* Cdc25C [16, 18].

Here, we have assessed the capacity of n-HPLC coupled to a linear IT to map the phosphorylation sites in a GST–Cdc25C recombinant protein containing residues 9–206 of the amino terminal region of *Xenopus* Cdc25C. The combined use of endopeptidase digestions with either trypsin or chymotrypsin and dual MS analysis of the resulting peptides, (DDNL [19] or TPIS [6, 12, 20, 21]), facilitated the comprehensive identification of the sites in Cdc25C phosphorylated by Cdc2–cyclin B *in vitro*.

2 Materials and methods

2.1 Protein expression and purification

GST-*Xenopus* Cdc25C (residues 9–206, Fig. 1) and GST-*Xenopus* Cdc2 recombinant proteins were expressed in *Escherichia coli* BL21 (DE3), as described previously [22]. Cells were harvested after induction with IPTG for 5 h at 25°C, washed with cold PBS and lysed in 50 mM Tris (pH 8), 0.5 M NaCl, 1 mM EDTA, 1 mM PMSF, 1 mM benzamidine, 1% Triton X-100 and 1 mg/mL lysozyme and protease inhibitors, for 15 min at 4°C. After sonication and centrifugation at $10\,000 \times g$ for 15 min, the supernatant was collected and mixed with glutathione–sepharose 4B beads (GE Healthcare) for 60 min at 4°C. The beads were washed with the same lysis buffer without Triton X-100 or lysozyme, and the GST-tagged recombinant proteins were eluted with 20 mM glutathione in 50 mM Tris (pH 8), 50 mM NaCl, 1 mM DTT, dialysed against 50 mM Tris (pH 8), 50 mM NaCl, 0.1 mM EDTA, 0.5 mM DTT, 5% glycerol and stored at −70°C until use [22]. The cyclin B protein used in this work was purified from Sf9 cells grown at 27°C for 48 h after infection with baculovirus encoding a His-tagged version of human cyclin B1, as described previously [23] (provided by Bill Dunphy and Akiko Kumagai, California Institute of Technology, Pasadena, USA). This cyclin B was isolated by harvesting the cells and lysing them in 50 mM $NaPO_4$ (pH 7.5), 150 mM NaCl, 0.05% Triton X-100, 1 mM PMSF, 1 mM pepstatin, 1 mM chymostatin, 1 mM leupeptin for 15 min at 4°C. After centrifugation at $10\,000 \times g$ for 10 min, the supernatant was mixed with Talon™ beads (BD Biosciences) for 30 min at 4°C. The beads were then washed in buffer containing 50 mM $NaPO_4$ (pH 7.5), and 300 mM NaCl and transferred to a gravity-flow column (BioRad). The His-tagged proteins were eluted with 50 mM $NaPO_4$ (pH 7.5), 300 mM NaCl and 150 mM imidazole and all the fractions containing purified proteins were dialysed for 8 h against 20 mM $NaPO_4$ (pH 7.5), 50 mM NaCl, 0.1 mM EDTA, 0.5 mM DTT, 5% glycerol and stored at −70°C.

>GST-tagged Cdc25 construct including residues 9 to 206

MSPILGYWKIKGLVQPTRLLLEYLEEKYEEHLYERDEG
DKWRNKKFELGLEFPNLPYYIDGDVKLTQSMAIIRYIA
DKHNMLGGCPERAEISMLEGAVLDIRYGVSRIAYSKDF
ETLKVDFLSKLPEMLKMFEDRLCHKTYLNGDHVTHPDF
MLYDALDVVLYMDPMCLDAFPKLVCFKKRIEAIPQIDK
YLKSSKYIAWPLQGWQATFGGGDHPPKSDLVPRGSEAP
PKTNTGLNFRTNCRMVLNLLREKDCSVTFSPEQPLTPV
TDLAVGFSNLSTFSGETPKRCLDLSNLGDETAPLPTES
PDRISSGKVESPKAQFVQFDGLFTPDLGWKAKKCPRGN
MNSVLPRLLCSTPSFKKTSGGQRSVSNKENEGELFKSP
NCKPVALLLPQEVVDSQFSPTPENKVDISLDEDCEMNI
LGSPGISGGGGGILDSMGRLELKLNSS

Figure 1. GST–Cdc25C recombinant protein sequence bearing the NH_2-terminal regulatory domain of *Xenopus* Cdc25C (residues 9–206 are underlined). The recombinant protein was expressed in *E. coli* and used as a model to map the phosphorylation sites after *in vitro* phosphorylation by Cdc2–cyclin B.

2.2 Formation of active Cdc2–cyclin B complexes

GST-Cdc2 (2 μg) purified from *E. coli* was incubated for 40 min at 22°C with 20 μL of interphase *Xenopus* egg extract (prepared as described by Murray [24]), to allow proper refolding of the Cdc2 recombinant protein [15, 25]. GST–Cdc2 was recovered using glutathione–sepharose 4B beads (GE Healthcare) and diluted ten-fold in H1K buffer (80 mM β-glycerophosphate [pH 7.5], 20 mM EGTA, 15 mM $MgCl_2$, 1 mM DTT, 1 mM PMSF, 2.5 mM benzamidine and 2 mg/mL each of leupeptin and aprotinin). Purified His-cyclin B (2 μg) was then added and incubated for 20 min at 22°C to obtain the active Cdc2–cyclin B complex.

2.3 *In vitro* phosphorylation of GST–Cdc25C

Purified GST–Cdc25C (15 μg) was phosphorylated *in vitro* for 2 h at 30°C by Cdc2–cyclin B (4 μg) in 40 μl of kinase buffer containing 1 mM ATP. Approximately, 8 μg (160 pmol) of control and phosphorylated GST–Cdc25C *per* lane was loaded on nondenaturing 12.5% PAGE gels [26] and visualized by CB staining. The kinase activity of Cdc2–cyclin B on GST–Cdc25C was tested by autoradiography. After incubating the protein with 2 μCi of radioactive [γ-^{32}P] ATP (3000 Ci/mmol) for 15 min at 30°C, samples were run in 12.5% SDS-PAGE by using a Hoeffer SE 600 device.

2.4 In-gel digestion

The bands corresponding to the nonphosphorylated (control) and *in vitro* phosphorylated Cdc25C were excised from the gels, washed, reduced in-gel and Cys-alkylated [27] before digesting with sequencing-grade trypsin (Promega), as described previously [28], or with chymotrypsin (Princeton Separations, Adelphia, USA). Chymotrypsin was resuspended in 50 mM Tris HCl (pH 8.0) in 1 mM $CaCl_2$, added at a ratio of 1:50 (enzyme/protein) and incubated at 30°C for 10 h. The supernatants were transferred to new tubes, dried using a SpeedVac and resuspended in 0.1% formic acid in water suitable for mass analysis.

2.5 Protein analysis by MS and database search

Peptides were eluted on an RP PepMap C18 column (75 μm id × 15 cm) (LC Packings, Amsterdam, The Netherlands) using a 60 min linear gradient from 5 to 60% solvent B, solvent A being 0.1% formic acid in water and solvent B 0.1% formic acid in ACN. All HPLC runs were performed using an Ultimate 3000 n-HPLC system (LC Packings) operated at the 300 nL/min constant flow rate. The peptides were scanned and fragmented with an LTQ linear IT spectrometer (ThermoFinningan, San Jose, CA, USA) equipped with a dynamic nano-ESI source. An electrospray voltage of 1700 V and a capillary voltage of 50 V at 190°C were used for both DDNL and TIPS analyses. The LTQ was operated in data-dependent ZoomScan and MS/MS switching mode using the five most intense precursors detected in survey scans ranging from 400 to 2000 m/z (3 μscans), with an isolation width of ± 1.5 U and 35% normalized collision energy. The following parameters were set for searches using TurboSequest™: enzyme, trypsin; fixed modifications, carboxyamidomethyl cysteine; variable modifications, oxidation of methionine; peptide tolerance, ± 1.50 amu; fragment ion tolerance, ± 0.35 amu; number of missed cleavage sites, 1. All fragmentation spectra were first searched against a local database containing 1360 entries from *Xenopus laevis* retrieved from Uniprot Knowledgebase version 8.3 updated on July 2006 (ftp://ftp.ebi.ac.uk/pub/databases/uniprot/current_release/knowledgebase) plus one extra entry with the recombinant protein of interest (Fig. 1). To address the false–positive rate in the database search using SEQUEST, we searched the same spectra against the *X. laevis* reversed database. The reverse database was created by reversing each individual protein sequence entry, such that the original sequence length and composition were preserved. The same parameters were used for chymotrypsin digestions but 'no enzyme' was specified as a variable and up to two missed cleavage sites were allowed. Only those peptides achieving $X_{corr} \geq 1.5$ for singly, 2.0 for doubly and 2.5 for triply charged peptides were considered.

For the analysis of the *in vitro* phosphorylated Cdc25C, the resulting tryptic and chymotryptic peptides were submitted to DDNL analysis using the same ESI-MS/MS conditions as above. The LTQ was programmed to trigger MS^3 fragmentation events on precursor ions with enhanced neutral loss (−98.0 for singly, −49.0 for doubly and −32.66 for triply charged peptides). All MS^2 and MS^3 spectra were manually inspected for diagnostic ions with phosphorylated residues.

All tryptic peptides that were more than four residues long and that included at least one Ser or Thr were considered for TPIS mass analysis. All the m/z ratios were calculated *in silico* including the mass of one potential phosphorylation event on the residues (indicated with an asterisk, *), and carboxyamidomethylation of Cys (indicated with ^) using GPMAW (Lighthouse Data, Denmark). Monoisotopic masses between 550 and 2000 calculated for peptides ranging from a charge state of +1 to +3 (a total of 21 precursor ions) were considered for TPIS analysis. This permitted the linear IT to selectively fragment all tryptic precursor ions ranging from 400 to 2000 m/z (3 μscans) that were detected in survey scans using the same ion isolation width and normalized collision energy as in DDNL acquisitions. The list of programmed monoisotopic m/z ratios, the corresponding tryptic sequence and z charge state for TPIS analysis are described in Table 1. Only one frequently observed peptide, containing one missed cleavage after Lys, was included. TPIS was only performed after the digestion of phosphorylated Cdc25C with trypsin, since it requires prior knowledge of the peptides corresponding to the protein of interest.

Table 1. Sequence and monoisotopic masses (theoretical monoisotopic masses were calculated considering the phosphorylation of one Ser/Thr residue) used in TPIS analysis after trypsin digestion of the Cdc25 recombinant protein

Sequence	*m/z*		
	$[M + H]^{+1}$	$[M + 2H]^{+2}$	$[M + 3H]^{+3}$
GSEAPPK	765.32	n. s.	n. s.
TNTGLNFR	1002.44	n. s.	n. s.
EK+DC^SVTFSPEQPLTPVTDLAVGFSNLSTFSGETPK	n. s.	1983.42	1322.61
DC^SVTFSPEQPLTPVTDLAVGFSNLSTFSGETPK	n. s.	1854.85	1236.90
C^LDLSNLGDETAPLPTESPDR	n. s.	1190.52	794.01
ISSGK	571.25	n. s.	n. s.
VESPK	639.27	n. s.	n. s.
AQFVQFDGLFTPDLGWK	n. s.	1024.98	683.66
GNMNSVLPR	1067.47	n. s.	n. s.
LLC^STPSFK	1132.50	566.75	n. s.
TSGGQR	685.27	n. s.	n. s.
SVSNK	614.25	n. s.	n. s.
SPNC^KPVALLLPQEVVDSQFSPTPENK	1537.74	1025.50	n. s.
VDISLDEDC^EMNILGSPGISGGGGGILDSMGR	n. s.	1651.22	1101.15
VDISLDEDC^EMNILGSPGISGGGGGILDSM^{OX}GR	n. s.	1659.22	1106.48

(+) missed cleavage of trypsin; (^) carboxyamidomethylation of cysteine; (ox) oxidation of methionine; n. s.: monoisotopic *m/z* ratio not scanned.

3 Results

3.1 *In vitro* phosphorylation of GST–Cdc25C

GST–Cdc25C was phosphorylated *in vitro* by Cdc2–cyclin B in the presence of ATP for 2 h at 30°C. Unphosphorylated and *in vitro* phosphorylated GST–Cdc25C were visualized in denaturing SDS-PAGE gels through CB staining (Fig. 2). The efficient phosphorylation of GST–Cdc25C was evident by the presence of a 50 kDa band in autoradiographs of the SDS-PAGE gels (Fig.2, lane 4).

3.2 Sequence coverage of the Cdc25C amino-terminus with the linear IT and two different endopeptidases

When the 198 residues of Cdc25C present in the fusion protein were considered, chymotrypsin digestion allowed for a better coverage of the protein sequence (91.9%) than trypsin digestion (77.7%). This was evident when equal amounts of protein (160 pmol) were submitted to mass analysis (Fig. 3). Among the 16 theoretical tryptic peptides within a mass range of a 400–6000 *m/z* ratio, the recombinant protein included fourteen different tryptic peptides with at least one Ser or Thr site that could possibly be phosphorylated. After trypsin digestion, three peptides containing either Ser or Thr were not detected. In contrast, due to the low cleavage specificity of chymotrypsin, 27 different peptides were generated. Among these, all the Ser and Thr residues present in the Cdc25 sequence were detected, except one Thr that was previously detected in one of the tryptic peptides.

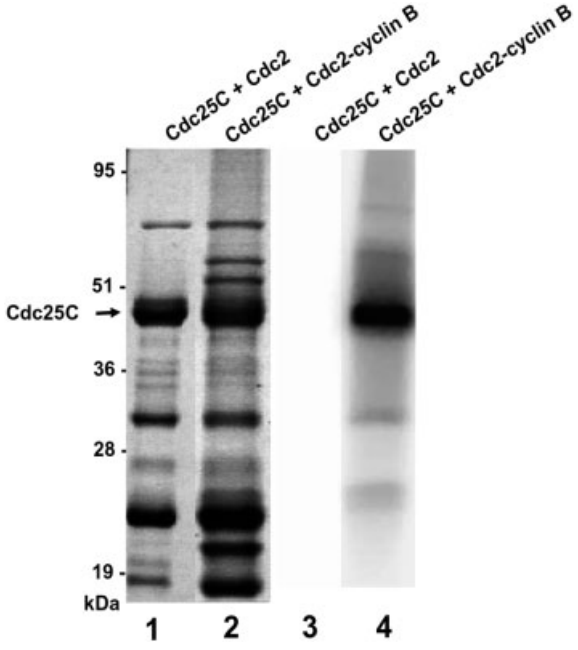

Figure 2. Phosphorylation of the N-terminus of Cdc25C by Cdc2–cyclin B *in vitro*. *E. coli*-derived GST-Cdc2 was incubated with a concentrated *X. laevis* oocyte extract and recovered on glutathione–sepharose beads. The beads were washed and incubated in the presence or absence of His-cyclin B prior to the addition of GST–Cdc25C and then with ^{32}P-γ-ATP. Coomassie-stained 12.5% SDS-PAGE gel corresponding to *X. laevis* GST–Cdc25C (N-terminus) recombinant protein before (lane 1) and after (lane 2) *in vitro* phosphorylation, respectively. Lanes 3 and 4 correspond to the autoradiography of the SDS-PAGE gels, revealing a band corresponding to phosphorylated Cdc25C in lane 4.

sequence coverage after tryptic digestion: **77.7%**

SEAPPKTNTGLNFR**TNCRMVLNLLREKDCSVTFSPEQPLTPVTD**
LAVGFSNLSTFSGETPKRCLDLSNLGDETAPLPTESPDRISSGK
VESPKAQFVQFDGLFTPDLGWKAKKCPR**GNMNSVLPRLLCSTPS**
FKKTSGGQR**SVSNKENEGELFKSPNCKPVALLLPQEVVDSQFSP**
TPENKVDISLDEDCEMNILGSP

sequence coverage after chymotryptic digestion: **91.9%**

SEAPPKTNTGLNFRTNCRM**VLNLLREKDCSVTFSPEQPLTPVTD**
LAVGFSNLSTFSGETPKRCLDLSNLGDETAPLPTESPDRISSGK
VESPKAQFVQFDGLFTPDLGWKAKKCPRGNM**NSVLPRLLCSTPS**
FKKTSGGQRSVSNKENEGELFKSPNCKPVALLLPQEVVDSQFSP
TPENKVDISLDEDCEMNILGSP

Figure 3. Cdc25 sequence coverage after trypsin (top) and chymotrypsin (lower) digestion. Peptides were identified by nano-LC–nano-ESI linear IT MS. The residues observed after each enzymatic digestion are shown in bold.

After searching against the *X. laevis* reverse database, no false–positives corresponding to the Cdc25 sequence were observed.

3.3 Phosphorylation site mapping with DDNL and TPIS analysis after tryptic digestion

Only three phosphopeptides were detected by DDNL after trypsin digestion compared to the six different phosphopeptides detected using TPIS, each with a single phosphorylated residue (Thr^{48}, Thr^{67}, Thr^{86}, Thr^{112}, Thr^{138} and Ser^{163}, respectively, Fig. 4 and Table 2). The small differences (from 0 to 1.12 amu) between the experimental and *in silico* calculated theoretical masses of the precursor ions indicate that the mass measurement of the precursor ion was very accurate. One of the six peptides detected in the TPIS analysis (AQFVQFDGLFT*PDLGWK) was also found after the DDNL analysis. Figure 5 shows MS^2 fragment spectra corresponding to two tryptic phosphopeptides. Figure 5A corresponds to the fragmentation spectrum of a phosphopeptide ($m/z = 978.60$) detected by DDNL analysis, whilst Fig. 5B shows the fragmentation spectrum of a phosphopeptide ($m/z = 517.70$) detected by TPIS analysis. Diagnostic ions bearing phosphorylations are indicated. m/z corresponding to the loss of one H_3PO_4 molecule from precursor ions are also indicated with arrows.

3.4 Phosphorylation site mapping with DDNL after digestion with chymotrypsin

Although less specific than trypsin, the cleavage of Cdc25C with chymotrypsin yielded more, smaller and distinct peptides to trypsin digestion, permitting a better coverage and analysis of the phosphorylation sites by DDNL. Examples of MS^3 (Fig. 6A) and MS^2 (Fig. 6B) fragmentation events from chymotryptic peptides are shown. In the former case, the occurrence of a phosphorylation on Thr^{138} can be inferred because of the presence of dehydroaminobutyric, due to the loss of H_3PO_4 from the precursor phosphorylated ion. Figure 6B corresponds to a doubly phosphorylated peptide. Two phosphorylated residues (Thr^{67} and Ser^{205}) were only identified after chymotrypsin digestion. The triply charged precursor ion $[M + 3H]^{+3}$ $m/z = 1182.86$ with sequence DLSNLGDETAPLPT*ESPDRISSGKVES*PKAQF bears two phosphate moieties on Thr^{86} and Ser^{99}. The experimental monoisotopic mass of the triply charged peptide $m/z = 1182.86$ only differs 0.32 amu from the theoretical monoisotopic mass calculated *in silico* for this peptide including the mass of two phosphate moieties ($m/z = 1182.54$) (Table 2). Figure 6B shows the loss of the two phosphate moieties as phosphoric acid in the MS^2 event, yielding two prominent neutral losses with m/z ratios 1150.30 and 1117.70, respectively. The occurrence of these neutral losses in the MS^2 spectrum from the precursor ion gives further evidence of the occurrence of a double phosphorylation in this specific peptide.

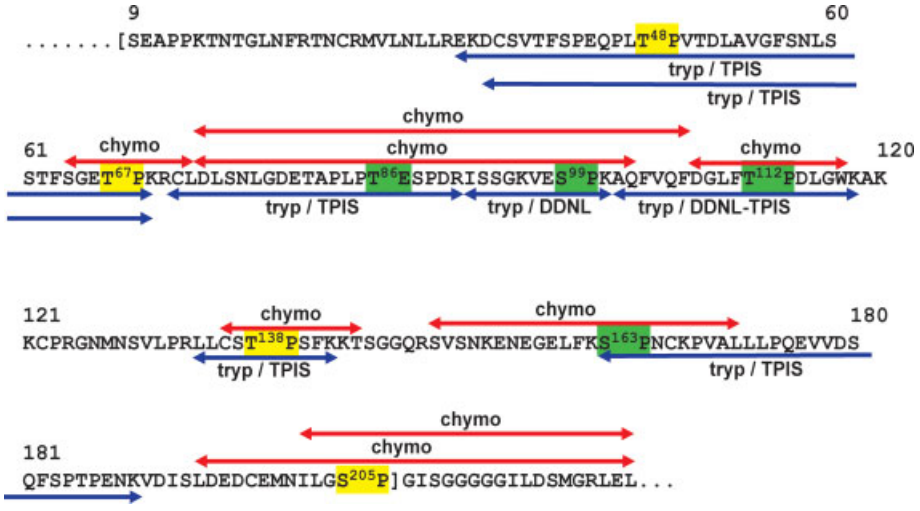

Figure 4. Trypsin (blue arrows) and chymotrypsin (red arrows) peptides bearing phosphorylated residues (position indicated in superscript). The sequence in brackets corresponds to Cdc25C. The four Cdc2–cyclin B phosphorylation sites previously described in Cdc25C (Thr^{48}, Thr^{67}, Thr^{138} and Ser^{205}) are shaded in yellow. The four novel phosphorylation sites found after endopeptidase digestion (Thr^{86}, Ser^{99}, Thr^{112} and Ser^{163}) are shaded in green. The kind of mass analysis used for the detection of every peptide, DDNL or TPIS, is also indicated.

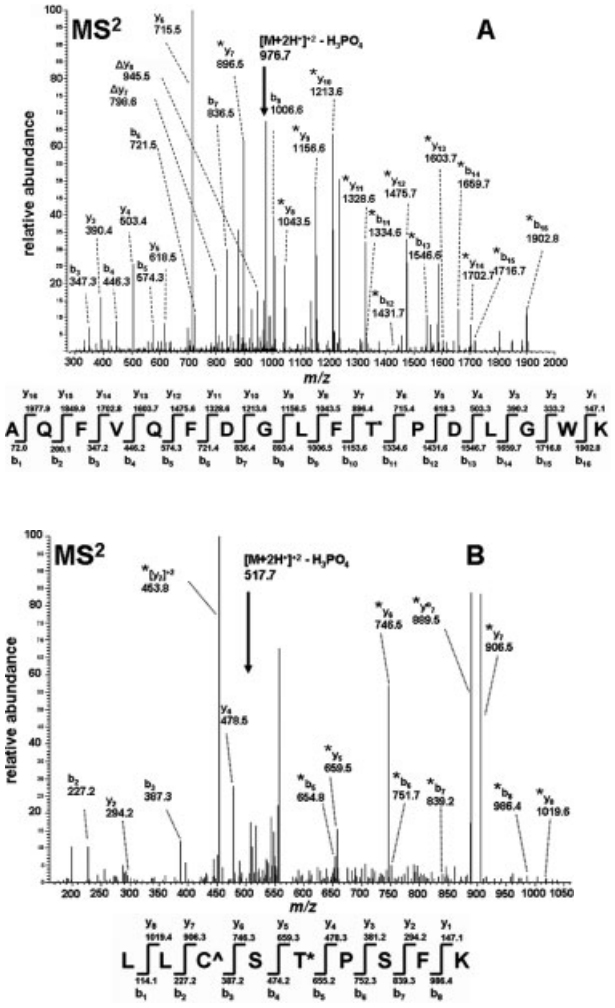

Figure 5. Identification of tryptic phosphopeptides by RP-HPLC with linear IT MS. (A) Fragmentation spectra corresponding to the ion at *m/z* 976.7, detected using data-dependent neutral loss (DDNL) and (B) at *m/z* 517.7 detected using TPIS mass analysis. Phosphorylated Ser and Thr residues are indicated by an asterisk (*). The peptide sequence and the assignment of the fragmentation series are also indicated. The expected ion masses have been listed above the sequence. Diagnostic ions bearing phosphate are indicated with an asterisk (*), whilst loss of phosphate from the ions is indicated by (Δ). Loss of water from a fragment ion is indicated with (°).

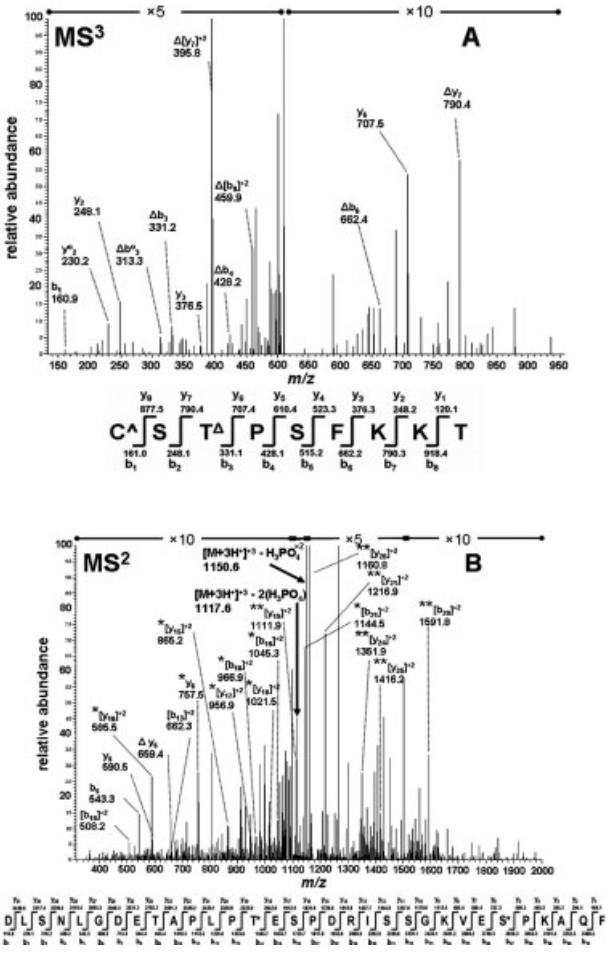

Figure 6. Identification of chymotrypsin phosphopeptides by RP-HPLC with linear IT MS. Fragmentation spectra corresponding to single (A) and dual (B) phosphorylated chymotrypsin peptides. (A) The fragmentation spectrum corresponds to an MS^3 event showing the presence of dehydroaminobutyric (T^{Δ}) due to the loss of H_3PO_4 from the phosphorylated precursor ion. (B) The triple-charged precursor ion $[M + 3H]^{+3}$ *m/z* = 1182.86 corresponds to the doubly phosphorylated peptide DLSNLGDETAPLPT*ESPDRISSGKVES*PKAQF. The loss of the two phosphoric acid molecules in the MS^2 event yielded two prominent neutral losses (black arrows) with *m/z* ratios of 1150.6 and 1117.6, respectively. The ions are labelled as in Fig. 5.

4 Discussion

Two alternative digestions of recombinant Cdc25C with trypsin and chymotrypsin, followed by the analysis of the resulting peptides with n-HPLC coupled online to a linear IT mass, yielded extensive sequence coverage of Cdc25, a prerequisite for the comprehensive mapping of phosphorylation sites. A total of eight different phosphorylated residues (Thr^{48}, Thr^{67}, Thr^{86}, Ser^{99}, Thr^{112}, Thr^{138}, Ser^{163} and Ser^{205}) were identified in the *in vitro* phosphorylated recombinant protein (Fig. 4). Five of the eight-phosphorylation sites (Thr^{86}, Ser^{99}, Thr^{112}, Thr^{138} and Ser^{163}) were identified in both the tryptic and chymotryptic peptides (Table 2), but two (phosphorylated Thr^{67} and Ser^{205}) were exclusively identified after the digestion with chymotrypsin. The phosphorylated Ser^{205} residue was not detected after trypsin digestion because the corresponding tryptic peptide VDISLDEDCEMNILGS*PGISGGGGGILDSMGR (where the Cdc25 sequence is underlined) could not be identified by the linear IT. This is in accordance with the lower sequence coverage of the trypsin analysis, although Thr^{48} could only be unambiguously identified after trypsin proteolysis.

Table 2. Phosphorylation sites found in recombinant GST–Cdc25C protein from *X. laevis* after endopeptidase digestion with trypsin and chymotrypsin

Tryptic peptides					Chymotryptic peptides			
Sequence	z [a]	m/z [b] exp./theor.	X_{corr} [c] DDNL	X_{corr} [d] TPIS	Sequence	z [a]	m/z [b] exp./theor.	X_{corr} [c] DDNL
34-EK+DC^SVTFSPEQPLT*PVTDLAVGFSNLSTFSGETPK-69	+3	1322.61/1322.61	n. d.	4.67	64-SGET$^{\Delta}$PKRC^L-72	+2	515.52/515.24	2.29
36-DC^SVTFSPEQPLT*PVTDLAVGFSNLSTFSGETPK-69	+3	1236.90/1236.90	n. d.	2.57	73-DLSNLGDETAPLPTESPDRISSGKVES*PKAQ-103	+3	1107.27/1106.86	3.86
71-C^LDLSNLGDETAPLPT*ESPDR-91	+3	794.01/794.01	n. d.	2.60	73-DLSNLGDETAPLPTESPDRISSGKVES$^{\Delta}$PKAQ-103	+3	1074.70/1074.26	3.86
92-ISSGK+VES$^{\Delta}$PK-101	+2	507.55/507.27	2.65	n. d.	73-DLSNLGDETAPLPT*ESPDRISSGKVESPKAQ-103	+3	1107.27/1106.86	3.29
102-AQFVQFDGLFT*PDLGWK-118	+2	1025.68/1024.98	5.59	5.51	73-DLSNLGDETAPLPT$^{\Delta}$ESPDRISSGKVESPKAQ-103	+3	1074.70/1074.26	3.80
102-AQFVQFDGLFT$^{\Delta}$PDLGWK-118	+2	976.43/975.98	4.92	n. d.	73-DLSNLGDETAPLPT*ESPDRISSGKVES*PKAQF-104	+3	1182.86/1182.54	4.12
134-LLC^ST*PSFK-142	+2	566.75/566.75	n. d.	2.01	73-DLSNLGDETAPLPT*ESPDRISSGKVES*PKAQFVQF-107	+3	1307.53/1307.27	4.67
163-S*PNC^KPVALLLPQEVVDSQFSPTPENK-189	+3	1025.49/1025.49	n. d.	3.72	108-DGLFT*PDLGW-117	+1	1201.62/1200.50	2.01
					108-DGLFT$^{\Delta}$PDLGW-117	+1	1102.56/1102.50	1.88
					136-C^ST$^{\Delta}$PSFKKT-144	+2	519.50/519.24	2.03
					150-SVSNKENEGELFKS*PNC^KPVAL-171	+3	843.41/843.06	3.46
					150-SVSNKENEGELFKS$^{\Delta}$PNC^KPVAL-171	+3	810.92/810.46	4.05
					194-LDEDC^EMNILGS*PGISGGGGGILDSM^{OX}GRLEL-224	+3	1087.05/1086.81	2.59
					202-ILGS*PGISGGGGGILDSM^{OX}GRLEL-224	+2	1126.82/1126.55	3.06

a) Predominant charge state (z) observed.

b) Experimental (exp.) and theoretical (theor.) mass-to-charge (m/z) ratios of precursor ions. Theoretical m/z values were calculated using GPMAW v 6.21 software.

c) Probability based score (X_{corr}) using DDNL analysis and Turbosequest search engine.

d) Probability based score (X_{corr}) using TPIS analysis and Turbosequest search engine.

(*) Increase of mass corresponding to the presence of a phosphorylation (PO_3^- = 80 amu) on Ser or Thr residues; (Δ) loss of mass corresponding to the phosphoric acid (H_3PO_4 = 98 amu) on Ser or Thr residues; (+) missed cleavage of trypsin; (^) carboxyamidomethylation of cysteine; (ox) oxidation of methionine; n. d.: not detected or low probability X_{corr}.

Seven out of eight phosphorylated residues were found in Cdc25C through DDNL analysis of the chymotryptic peptides, whilst only two different phosphorylation sites could be identified in the trypsin digest using the same analysis. Chymotryptic digestion was especially valuable to identify phosphorylated Thr^{86}, which is the only one that does not correspond to a canonical Ser/Thr–Pro phosphorylation site [29]. The Cdc2–cyclin B complex is a proline-directed Ser/Thr protein kinase [15]. Indeed, all the phosphorylated residues previously described in both *Xenopus* Cdc25C [18] and its human homologue [16, 17] are consensus Ser/Thr–Pro sites, whereas Thr^{86} corresponds to a Pro–Thr sequence. Our *in vitro* phosphorylation results indicate that the presence of Pro before Thr could also be recognized by Cdc2–cyclin B. Significantly, the phosphorylated Thr^{86} is followed by a Glu residue, fulfilling the requirements of polar/basic residues after phosphorylation sites described for different Cdc2–cyclin B substrates [30].

The phosphorylation on Thr^{48} was only detected after TPIS analysis of the tryptic peptides. Whilst DDNL analysis is a straightforward method for the detection of phosphopeptides, the main advantage of TPIS analysis is that it can be used to detect minimal amounts of phosphopeptides. However, TPIS requires prior knowledge of mass, predominant charge state and missed cleavage of the tryptic peptides that correspond to the protein of interest in the experimental conditions employed.

It has been shown that recombinant Cdc25C mutated on residues Thr^{48}, Thr^{67} and Thr^{138} display reduced phosphatase activity [16]. Moreover, the mutated Cdc25C showed significantly less electrophoretic retardation in SDS-PAGE gels, in contrast to wt Cdc25C that normally undergoes a significant electrophoretic mobility shift upon activation. Our results identified four additional Cdc25C residues (Thr^{86}, Ser^{99}, Thr^{112} and Ser^{163}) that could potentially be phosphorylated by Cdc2–cyclin B. Site-directed mutagenesis should validate the importance of these new Cdc25C phosphorylation sites.

Due to the increase in protein coverage following chymotrypsin digestion and the detection of low abundant ions by TPIS, the MS approach described here should be useful for the analysis of phosphorylation patterns in proteins with low stoichiometric levels of phosphorylated peptides and/or tryptic peptides outside the mass range detection limit (*i.e.* with too low or too high m/z ratios). Moreover, the four novel *in vitro* phosphorylated sites that we report here may help to unravel the fine regulation of MPF activity and its role in the G_2 to M transition of the cell cycle.

We thank A. Núñez for their technical assistance and Dr. Jesús Vázquez (CBM-CSIC) for helpful discussions regarding the TPIS methodology. The CNIO was partially supported by the RTICC (Red de Centros de Cáncer, FIS C03/10).

5 References

[1] Arrigoni, G., Resjo, S., Levander, F., Nilsson, R. *et al.*, *Proteomics* 2006, *6*, 757–766.

[2] Kumagai, A., Dunphy, W. G., *Cell* 1992, *70*, 139–151.

[3] Mann, M., Jensen, O. N., *Nat. Biotechnol.* 2003, *21*, 255–261.

[4] Mann, M., Hendrickson, R. C., Pandey, A., *Annu. Rev. Biochem.* 2001, *70*, 437–473.

[5] Meng, F. Y., Forbes, A. J., Miller, L. M., Kelleher, N. L., *Mass Spectrom. Rev.* 2005, *24*, 126–134.

[6] Villar, M., Ortega-Perez, I., Were, F., Cano, E. *et al.*, *Proteomics* 2006, *6*, S16–S27.

[7] Elias, J. E., Haas, W., Faherty, B. K., Gygi, S. P., *Nat. Methods* 2005, *2*, 667–675.

[8] Larsen, M. R., Thingholm, T. E., Jensen, O. N., Roepstorff, P., Jorgensen, T. J. D., *Mol. Cell. Proteomics* 2005, *4*, 873–886.

[9] Beausoleil, S. A., Jedrychowski, M., Schwartz, D., Elias, J. E. *et al.*, *Proc. Natl. Acad. Sci. US A.* 2004, *101*, 12130–12135.

[10] Olsen, J. V., Blagoev, B., Gnad, F., Macek, B. *et al.*, *Cell* 2006, *127*, 635–648.

[11] Steen, H., Jebanathirajah, J. A., Rush, J., Morrice, N., Kirschner, M. W., *Mol. Cell. Proteomics* 2006, *5*, 172–181.

[12] Salek, M., Alonso, A., Pipkorn, R., Lehmann, W. D., *Anal. Chem.* 2003, *75*, 2724–2729.

[13] Han, S. J., Conti, M., *Cell Cycle* 2006, *5*, 227–231.

[14] Nilsson, I., Hoffmann, I., *Prog. Cell Cycle Res.* 2000, *4*, 107–114.

[15] Strausfeld, U., Fernandez, A., Capony, J. P., Girard, F. *et al.*, *J. Biol. Chem.* 1994, *269*, 5989–6000.

[16] Izumi, T., Maller, J. L., *Mol. Biol. Cell* 1993, *4*, 1337–1350.

[17] Izumi, T., Walker, D. H., Maller, J. L., *Mol. Biol. Cell* 1992, *3*, 927–939.

[18] Perdiguero, E., Nebreda, A. R., *Cell Cycle* 2004, *3*, 733–737.

[19] Schlosser, A., Pipkorn, R., Bossemeyer, D., Lehmann, W. D., *Anal. Chem.* 2001, *73*, 170–176.

[20] Konig, S., Zeller, M., Peter-Katalinic, J., Roth, J. *et al.*, *J. Am. Soc. Mass Spectrom.* 2001, *12*, 1180–1185.

[21] Murray, K. K., Boyd, R. K., Eberlin, M. N., Langley, G. J. *et al.*, *Abstr. Pap. Am. Chem. Soc.* 2005, *229*, U123.

[22] Palmer, A., Gavin, A. C., Nebreda, A. R., *EMBO J.* 1998, *17*, 5037–5047.

[23] Kumagai, A., Dunphy, W. G., *Methods Enzymol.* 1997, *283*, 564–571.

[24] Murray, A. W., *Methods Cell Biol.* 1991, *36*, 581–605.

[25] Nebreda, A. R., Gannon, J. V., Hunt, T., *EMBO J.* 1995, *14*, 5597–5607.

[26] Anderson, C. W., Baum, P. R., Gestelan, R. F., *J. Virol.* 1973, *12*, 241–252.

[27] Herbert, B., Galvani, M., Hamdan, M., Olivieri, E. *et al.*, *Electrophoresis* 2001, *22*, 2046–2057.

[28] Shevchenko, A., Wilm, M., Vorm, O., Mann, M., *Anal. Chem.* 1996, *68*, 850–858.

[29] Nigg, E. A., *Curr. Opin. Cell Biol.* 1993, *5*, 187–193.

[30] Moreno, S., Nurse, P., *Cell* 1990, *61*, 549–551.

